

THE ORIGIN OF ENHANCED ACTIVITY IN THE SUNS OF M67

A. REINERS¹

Institut für Astrophysik, Georg-August-Universität, Friedrich-Hund-Platz 1, 37077 Göttingen, Germany

AND

M.S. GIAMPAPA

National Solar Observatory², National Optical Astronomy Observatory², 950 North Cherry Avenue, P.O. Box 26732, Tucson, AZ 85726-6732

Draft version November 23, 2018

ABSTRACT

We report the results of the analysis of high resolution photospheric line spectra obtained with the UVES instrument on the VLT for a sample of 15 solar-type stars selected from a recent survey of the distribution of H and K chromospheric line strengths in the solar-age open cluster M67. We find upper limits to the projected rotation velocities that are consistent with solar-like rotation (i.e., $v \sin i \lesssim 2\text{--}3 \text{ km s}^{-1}$) for objects with Ca II chromospheric activity within the range of the contemporary solar cycle. Two solar-type stars in our sample exhibit chromospheric emission well in excess of even solar maximum values. In one case, Sanders 1452, we measure a minimum rotational velocity of $v \sin i = 4 \pm 0.5 \text{ km s}^{-1}$, or over twice the solar equatorial rotational velocity. The other star with enhanced activity, Sanders 747, is a spectroscopic binary. We conclude that high activity in solar-type stars in M67 that exceeds solar levels is likely due to more rapid rotation rather than an excursion in solar-like activity cycles to unusually high levels. We estimate an upper limit of 0.2% for the range of brightness changes occurring as a result of chromospheric activity in solar-type stars and, by inference, in the Sun itself. We discuss possible implications for our understanding of angular momentum evolution in solar-type stars, and we tentatively attribute the rapid rotation in Sanders 1452 to a reduced braking efficiency.

Subject headings: open clusters and associations: individual (M67, NGC 2682) — stars: activity — stars: rotation — stars: chromospheres — Sun: activity

1. INTRODUCTION

In a survey of the Ca II H and K core strengths of a sample of 60 solar-type stars in the solar-age, solar-metallicity open cluster M67, Giampapa et al. (2006) found that the distribution of the HK index – a measure of the strength of the chromospheric H and K cores – is broader than the distribution seen in the contemporary solar cycle. Significant overlap between the HK distribution of the solar cycle and that for the sun-like stars in M67 is seen with over 70% of the solar analogs exhibiting Ca II H+K strengths within the range of the modern solar cycle. About $\sim 10\%$ are characterized by high activity in excess of solar maximum values while approximately 17% have values of the HK index less than solar minimum.

In view of these results, a key question that arises is whether the distribution of the HK index in M67, and especially the occurrence of solar-type stars in this cluster with levels of activity exceeding solar maximum, is due to excursions in the amplitude of otherwise solar-like cycles or whether the high HK values in some solar-type members are simply the result of their more rapid rotation. The former possibility is reminiscent of the

prolonged episode of quiescence known as the Maunder Minimum where sunspots vanished, coinciding with the Little Ice Age (Foukal & Lean 1990), as well as the extended period of high solar activity, as inferred from isotopes in the terrestrial record, known as the Medieval Solar Maximum during the so-called Medieval Warm Epoch (Jirikovic & Damon 1994). In the case of the latter possibility of more rapid rotation, we know that atmospheric activity associated with surface magnetic fields, in general, increases with increasing equatorial rotation velocity in late-type stars (e.g., Skumanich 1972; Pallavicini et al. 1981; Baliunas et al. 1995; Pizzolato et al. 2003).

The presence of active solar-type stars in the solar-age cluster M67 is particularly surprising. It is therefore crucial to determine whether it is rapid rotation that is the origin of the relatively enhanced activity, or if the rotation of these objects is solar-like but their cycle variations extend to relatively higher amplitudes than seen in the Sun. If it is more rapid rotation that is the natural origin of the higher Ca II core emission then this result would invite further investigation of the angular momentum evolution of M67 in contrast to that of the more slowly rotating Sun and other solar-age G dwarfs. However, if rotation velocities are solar-like at $\sim 2 \text{ km s}^{-1}$ then this would suggest that excursions in the cycle variation of solar-type stars that are significantly in excess of contemporary solar maximum values can occur in Sun-like stars and, by implication, in the Sun itself. We therefore discuss in this investigation the results of our attempt to measure projected rotation velocities in selected

Electronic address: Ansgar.Reiners@phys.uni-goettingen.de

Electronic address: giampapa@noao.edu

¹ Emmy Noether Fellow

² The National Solar Observatory and the National Optical Astronomy Observatory are each operated by the Association of Universities for Research in Astronomy, Inc. (AURA) under respective cooperative agreements with the National Science Foundation

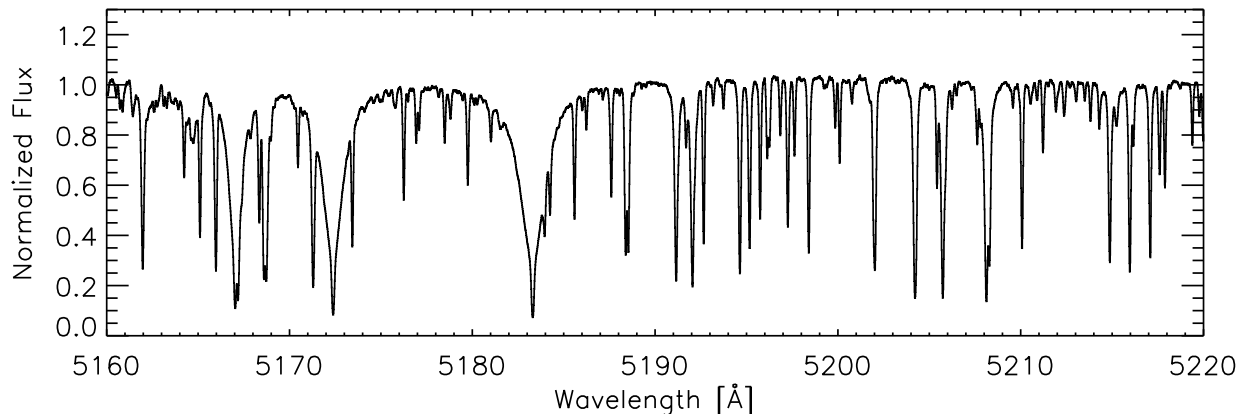


FIG. 1.— Spectral window of our Ganymede spectrum.

M67 solar-type stars from the sample of Giampapa et al. (2006). The sample selection and the acquisition of the observations are discussed in §§2-3 while the novel approach to the analysis is given in §4. The results are presented in §5 and a discussion followed by our conclusions are given in §§6 and 7, respectively.

2. SAMPLE SELECTION

We selected a sample of 15 sun-like stars from Giampapa et al. (2006). Our targets cover a range in $B - V$ of 0.62–0.67, which corresponds to spectral types G2–G6 or effective temperatures of 5700–5850 K (Kenyon & Hartmann 1995). Giampapa et al. (2006) found that the majority of stars in M67 exhibits Ca H&K emission similar to the Sun; most of their targets populate the range 155–260 mÅ in HK index. As defined in Giampapa et al. (2006), this index is the sum of the relative intensities in 1 Å bandpasses centered at the H and K lines in the calibrated spectrum. Two outliers with exceptionally strong Ca II emission were found, Sanders 747 (354 mÅ) and Sanders 1452 (414 mÅ). Our sample consists of 13 stars with HK indices similar to the Sun plus the two stars with higher HK indices. Additionally, we obtained a spectrum of the Sun through the same instrumental setup by observing its light reflected from Jupiter’s moon Ganymede.

3. DATA

The data were obtained using ESO’s high resolution spectrograph UVES at the VLT in its red arm centered at 580 nm. This setup covers the wavelength range 480 nm to 680 nm on two chips with a gap at 575–585 nm. To achieve the highest possible spectral resolution, we used the image slicer #3 providing a resolving power of $R \sim 110\,000$. After exposure times between 30 min and 1 h per star, the spectra from the blue chip have signal-to-noise ratios of about 40 per resolution element. The spectrum of Ganymede attained a SNR above 400 after 20 s. A part of our Ganymede spectrum from the blue chip is shown in Fig. 1.

The part of the spectrum obtained on the red chip unfortunately is compromised by an interference pattern which is most likely related to electronic noise. Such an interference pattern with a peak-to-peak amplitude of about 1 ADU was present from the beginning of UVES

operations³. In our case, the reason for the noise pattern seems to be related to the interference pattern, but in our data the noise has grown much larger. This pattern is difficult to correct for, and we decided not to use data from the red chip for our analysis; the available spectral range on the blue chip carries sufficient information and the red part is not crucial for our purpose.

4. ANALYSIS

At a SNR of 40 and a resolving power of $R \sim 110\,000$, i.e. $\Delta v \sim 2.7 \text{ km s}^{-1}$, the difference between sun-like stars rotating at 2 km s^{-1} and 4 km s^{-1} cannot be detected with high confidence. The main obstacle is the large intrinsic width of spectral lines in sun-like stars, which due to temperature broadening and turbulent motions have FWHM exceeding 6 km s^{-1} (e.g. Gray 2005). Thus, at a sampling rate slightly better than 3 km s^{-1} , the difference between additional rotational broadening of 2 and 4 km s^{-1} is very subtle.

To overcome the relatively low SNR, we derive a mean line broadening over a large spectral range including several hundred spectral lines (see also Reiners & Schmitt 2003a,b). By performing a least-squares deconvolution process, we search for line broadening that is common to all lines that we take into account. In other words, we search for the broadening function that, applied to a template spectrum of unbroadened spectral lines, produces the best fit to our data. As a template, we start with a “ δ -template” that is non-zero only at the position of spectral lines and zero elsewhere (for technical reasons, we do not fit to the normalized spectrum $f(\lambda)$, but to $1 - f(\lambda)$ instead). The intensity at the position of spectral lines is estimated from the modelled central line depth taken from the Vienna Atomic Line Database (VALD, Kupka et al. 1999). Before the deconvolution process, we apply a “thermal” broadening to each line in the template, i.e., we convolve each line with a Gaussian according to the expected motion of the gas at given atomic mass and gas temperature. This broadening is different between lines of different atoms and hence has to be included before the deconvolution. With this template in hand, we search for the function that, convolved with our template, provides the best fit to the data. In

³ We thank the ESO user support department for their help with the data. A replacement of the red chip of UVES is foreseen in May 2009.

this function, each of the typically 60–80 pixels is a free parameter.

It is important to realize that the described analysis is mainly a technical procedure. We do not model the full set of parameters relevant for spectral line broadening, which include for example turbulence velocities, temperature structure and density stratification. Instead, we assume that our sample stars have atmospheres that are approximately the same at least on the level interesting for this analysis, and that the main difference in spectral line width is due to rotation.

We utilize in our analysis the spectral range 5400–5750 Å, where more than 300 spectral lines in this region are included in the fit. In order to accurately recover the shape of the broadening function, it is important that the equivalent widths of the spectral lines are chosen correctly. Equivalent widths are estimated from VALD data in the first step, but this usually does not provide an adequate set of lines. Moreover, at this level of accuracy, stars are very different in the distribution of line depths. We adjust for the distribution of line depths by an iterative procedure fitting line depths and broadening function alternately. This means that after the initial deconvolution described above, we run the same fitting procedure but now we fit for all line depths instead of the broadening function, which we keep fixed. With the new set of line depths we repeat the fitting of the broadening function and so forth until a stable solution is reached.

4.1. The broadening function of the Sun

In order to test our deconvolution procedure on real data, we applied the very same process to the solar flux atlas provided by NSO/NOAO ($R \sim 400,000$, Kurucz et al. 1999), and we observed the Sun with UVES using the same instrument setup as for our M67 targets. This was done because the effect of our deconvolution procedure on spectra from very slow rotators is not straightforward to estimate. In particular, this test reveals whether any spurious broadening is introduced by the deconvolution process. Furthermore, we use this test to investigate the influence of the UVES image slicer on the line broadening. The results of the deconvolution procedure in the two solar spectra are shown in Fig. 2.

First, one can see that the deconvolution process produces a smooth broadening function with a FWHM of roughly 6 km s^{-1} from the solar flux atlas (thin solid line). The wings of this function are relatively broad extending out to $\pm 10 \text{ km s}^{-1}$. We compared this profile to a few absorption lines in the spectrum finding that the line width and shape of the broadening profile does not significantly differ from those of individual lines. At a rotation velocity of $v \sin i = 1.8 \text{ km s}^{-1}$, the main effect of line broadening comes from turbulent gas motion. This effect is well known and should not be further studied here, but it is important to realize that even at very high spectral resolution, the slow rotation of the Sun is barely detectable in its spectrum.

The broadening profile of the Sun seen through the UVES instrument is also shown in Fig. 2 (thick grey line). As expected, it is somewhat broader than the one from the solar flux atlas. We artificially broadened the broadening function from the solar flux atlas to the spectral resolving power of UVES ($R \sim 110,000$). The result is

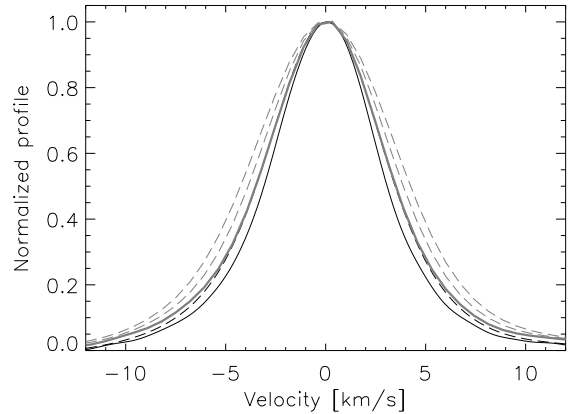


FIG. 2.— Broadening function of the Sun from the solar flux atlas (thin solid line). Thick grey line: Ganymede broadening function from UVES observations. Thin black dashed line: Broadening function from the solar flux atlas (thin solid line) artificially broadened by a Gaussian instrumental profile with $R=110,000$. Dashed grey lines: Ganymede broadening function artificially broadened to show a Sun rotating at 3 and 4 km/s .

overplotted as a black dashed line in Fig. 2. This line resembles remarkably well the broadening profile derived from our UVES observations (the small difference beyond $\pm 6 \text{ km s}^{-1}$ is probably an effect of the image slicer). Thus, we are confident that the UVES instrument does not introduce additional broadening on a scale that is relevant for our investigation. Note that the difference between the broadening profiles introduced by spectral resolutions that differ by about a factor of ten ($\sim 10^6$ for the solar flux atlas and $\sim 10^5$ for UVES) is relatively little. This is another consequence of the strong broadening due to turbulence, which at a resolution of $R \sim 110,000$ is already sampled quite well.

4.2. The effect of rotation

To display the effect of rotation on the broadening functions in sun-like stars, we artificially broadened the spectrum of Ganymede to construct the broadening function of a sun-like star rotating at projected velocities of $v \sin i = 3$ and 4 km s^{-1} . Artificial broadening is done by a convolution of the spectrum with a broadening function $G(v)$ (e.g., Eq. (18.14) in Gray 2005). We took into account the fact that the Sun is rotating ($v \sin i \sim 1.8 \text{ km s}^{-1}$), i.e., we approximate rotational broadening as a net effect of two consecutive broadening steps. The total broadening of $v \sin i$ given by the quadratic sum of two individual steps. In our case, the two steps are (1) the broadening introduced by solar rotation, and (2) a “reduced” artificial broadening. In other words, we use $v \sin i_{\text{reduced}} = \sqrt{(v \sin i)^2 - (1.8 \text{ km s}^{-1})^2} = 2.4$ and 3.6 km s^{-1} for the cases of $v \sin i = 3$ and 4 km s^{-1} , respectively. We note that quadratically adding rotation velocities is only an approximation; the result of two artificial broadening processes cannot be described by one ($G(v_1) * G(v_2) \neq G(v_3)$). However, we are mainly interested in the differential comparison between the profiles. The correction we apply to the absolute rotational velocity is on the order of 10%, and we estimate that the differential error introduced by the imprecise treatment of consecutive rotations is on the order of 1% or less.

The two cases of $v \sin i = 3$ and 4 km s^{-1} are shown in Fig. 2 as grey dashed lines. They are clearly distinguish-

TABLE 1
RESULTS

Sanders Number	$(B - V)_0$	HK [mÅ]	$v \sin i$ [km/s]
746	0.66	209	—
747	0.65	354	SB2
770	0.63	195	—
777	0.63	208	—
785	0.65	221	—
802	0.67	193	—
991	0.63	179	—
1048	0.64	188	—
1106	0.67	168	—
1203	0.67	218	—
1218	0.63	194	—
1246	0.64	187	—
1452	0.62	414	4 ± 0.5
1462	0.63	193	—
1477	0.67	181	—

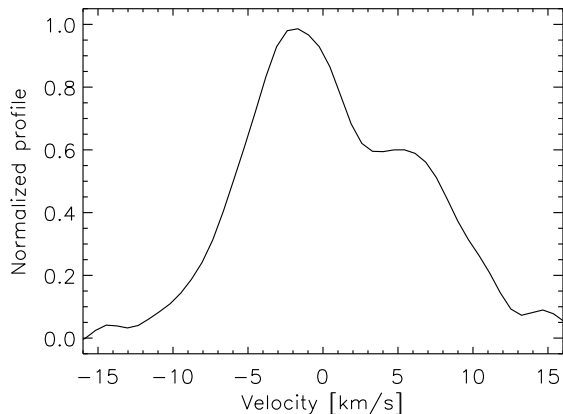


FIG. 3.— Broadening function of the spectroscopic binary Sanders 747.

able, which demonstrates that it is possible to differentiate between rotational broadening of 2, 3, and 4 km s⁻¹ in our data.

5. RESULTS

As explained in the former sections, we derived the broadening functions of all 15 members of M67 that we observed along with that for the Sun. In all cases, the iteration process converged to a stable solution providing a smooth broadening function. The stars of our sample and the solutions from our analysis are summarized in Table 1. Two stars of our sample show exceptionally high activity, i.e., a Ca HK index higher than 300 mÅ. The principal result of our analysis is that these two stars also show peculiar broadening functions. All other stars exhibit activity indices consistent with solar values observed during the solar activity cycle. These stars have broadening functions resembling the solar one implying they are consistent with very slow rotation, i.e., $v \sin i \lesssim 2$ km s⁻¹.

5.1. The spectroscopic binary Sanders 747

The first star that shows a peculiar broadening function is Sanders 747. We show the broadening function in Fig. 3. It clearly resembles the shape of a spectroscopic binary profile. Because both components are seen in

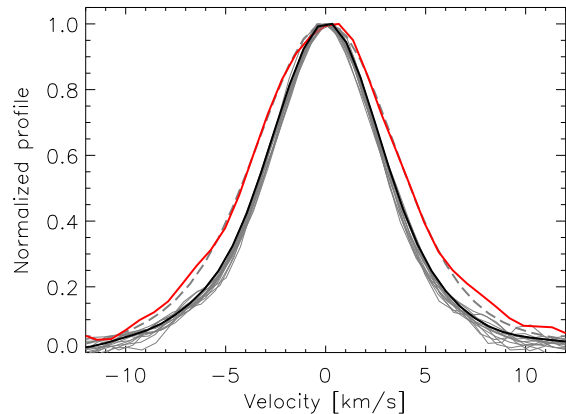


FIG. 4.— Broadening profiles of M67 stars (thin grey lines and thick red line) and of the Sun through Ganymede (thick black line). Dashed grey line: Ganymede spectrum artificially broadened to reproduce a $v \sin i = 4$ km s⁻¹ star (the same as the widest line in Fig. 2).

the deconvolved broadening function, their spectral types cannot be too different (otherwise one of the components would not be visible because it would not display lines at the positions of the template). The components have different maximum intensities, which could either mean that one component is brighter (or has more lines matching the template), or that one component is more rapidly rotating causing shallower lines. In fact, the slope of the stronger component (left wing of the broadening function) is steeper than the slope of the weaker component (right wing). This probably indicates a higher rotation velocity in one of the components. This high rotation velocity could be the reason for the enhanced activity observed in Sanders 747, but interactions between the two binary components may also be responsible through other mechanisms.

5.2. Rapid rotation in Sanders 1452

The broadening functions of all single stars of our sample are shown in Fig. 4. Thin grey lines show those of stars that are consistent with very slow rotation ($v \sin i \lesssim 2$ km s⁻¹). It is remarkable that all 13 profiles match each other very closely. They also closely resemble the broadening function of the Sun (Ganymede, thick black line).

The only star exhibiting a broadening function that is significantly wider than the others is Sanders 1452 (red line). We have overplotted an artificially broadened profile resembling a star rotating at $v \sin i = 4$ km s⁻¹ (grey dashed line, which is identical to the widest profile shown in Fig. 2). The profile expected from a star rotating at $v \sin i = 4$ km s⁻¹ is a very good match to the profile of Sanders 1452, with only the far wings beyond ± 6 km s⁻¹ differing slightly. This again may be an effect of the image slicer, but the far wings of the deconvolved broadening function are also less well defined due to the existence of uncaptured line blends and limited SNR in the data.

From the close match between the broadening function of Sanders 1452 and the artificially broadened versions of the Ganymede spectrum, we derive a value for the projected rotation velocity of Sanders 1452 of $v \sin i = 4 \pm 0.5$ km s⁻¹. The uncertainty is an empirical estimate deduced from a comparison with broadening functions with different values of $v \sin i$. Broadening

functions with $v \sin i = 3.5$ and 4.5 km s^{-1} can be distinguished from the data.

6. DISCUSSION

The results of our detailed spectroscopic analysis enable us to discuss the range of chromospheric activity seen in M67 in conjunction with the additional information on rotation, at least for a representative subset of solar-type stars in M67. We therefore briefly discuss in the following some relevant issues in this context, namely, (1) the potential range of brightness variability in sun-like stars at solar age and, by inference, in the Sun itself, and (2) some facets of angular momentum evolution in solar-type stars, including the possible origin of relatively rapid rotation at the age of the M67 open cluster.

6.1. *The Range of Activity and Brightness Variability in Sun-like Stars*

The potential excursions of the activity cycles of the M67 solar-like stars and possibly the Sun itself to exceptionally high values, as inferred from the HK distribution of the M67 solar-type stars given in Giampapa et al. (2006, their Fig. 3), now must be considered in the light of the rotation measures and estimates given herein. In particular, since S1452 with a mean HK index of $414 \text{ m}\text{\AA}$ is rotating at more than twice the equatorial solar rotation velocity, and S747 with a mean $\text{HK} = 354 \text{ m}\text{\AA}$ is a spectroscopic binary, the implication is that excursions in the cycles of M67 solar-type stars and the Sun itself appear to be less than about $\text{HK} \sim 250 \text{ m}\text{\AA}$, i.e., the next highest HK index found in the Giampapa et al. sample, which is roughly 10% higher than the representative maximum value seen in the modern solar cycle of $\text{HK} \approx 225 \text{ m}\text{\AA}$. Within the reported $B - V$ color range of the Sun of about 0.63 to 0.67 (VandenBerg & Bridges 1984), the only star in the Giampapa et al. sample that exceeds the maximum solar HK index (S 1014) also is a short-period binary with a period of 16.2 days and mean $\text{HK} = 248 \text{ m}\text{\AA}$. The determination of a definitive upper-limit to the HK index for single sun-like stars at solar age and metallicity will require a more extensive survey of rotation in the M67 solar-type stars.

Given our results and the well-known correlation between variations in chromospheric emission and changes in the solar irradiance or, correspondingly, in stellar brightness, it is of interest to consider the implications of the plausible upper limit to chromospheric emission in solar-type and solar-age stars, as inferred from the M67 sample, for the possible range of brightness variability that may occur. Using the color-dependent calibration approach described in Giampapa et al. (2006) and adopting a color of $B - V = 0.65$ as representative of analogs of the Sun, we find that the upper limit given above of $\text{HK} \simeq 250 \text{ m}\text{\AA}$ corresponds to $\log R'_{\text{HK}} \sim -4.70$, where R'_{HK} is the ratio of the total chromospheric H and K emission core flux to the stellar bolometric flux, corrected for the non-chromospheric (photospheric) contribution. Inspection of the results of long-term, high precision photometry of solar-type stars by Lockwood et al. (1997, their Fig. 17) as a function of the parameter R'_{HK} suggests that this level of activity would correspond to an annual mean level of rms brightness variations of roughly 0.002 mag, i.e. 0.2% variability in the brightness as recorded

in the Strömgren b and y bands, or about twice the $\sim 0.1\%$ variation in total irradiance that has been measured thus far for the contemporary Sun during the solar cycle. Therefore, we suggest that $\sim 0.2\%$ represents an upper limit to the likely excursion of the solar luminous output as a result of enhanced levels of magnetic activity.

We can refine this estimate of the upper limit further by noting that the brightness changes given by Lockwood et al. (1997) were for the mean variation of the sum of the Strömgren b and y bands. Hence, the variation of the total irradiance must be less than what is observed in these visible spectral bands. Radick et al. (1998) estimated (for small variations) a factor for converting between a fractional change in bolometric flux into the corresponding magnitude difference in $(b + y)/2$. Adopting their conversion factor of 1.39 and the estimate of brightness variations of 0.002 mag given above yields an estimate of 0.14% for the upper limit for variations in the bolometric flux. This is only slightly larger than the mean variation of 0.1% in the total solar irradiance observed during the course of the solar cycle.

6.2. *Angular Momentum Evolution in M67*

The relatively more rapid rotation of S1452 invites further consideration in the context of angular momentum evolution and the determination of stellar ages based on rotation, known as "gyrochronology" (Barnes 2007). At its measured (projected) rotation velocity and assuming a stellar radius close to solar, the "gyro-age" of Sanders 1452 is $1.0 \pm 0.2 \text{ Gyr}$ (Barnes 2007). This value is an upper limit because we measure only the projected velocity $v \sin i$. A more direct comparison can be obtained with the $v \sin i$ -age correlation given by Pace & Pasquini (2004, their Fig. 9). The inferred age (upper limit) of S1452 based on the three possible power law fits adopted by Pace & Pasquini is in the range of 1.2–1.5 Gyr. In either approach, the rotation-based age estimate for S1452 is in vivid contrast to the age range for M67 of 3.5–4.8 Gyr (Yadav et al. 2008) or that of the Sun, namely, 4.57 Gyr (e.g., Bonanno et al.; Baker et al. 2005) and the similar solar age implied for the slow rotators of our sample.

Given its higher rotational velocity, S1452 therefore represents an alternative path for angular momentum evolution among single stars in this solar-age cluster. In view of the relevance to the calibration of age-rotation laws and even the applicability of age-rotation relations to individual objects, a discussion of our results in the context of rotational evolution is merited.

In brief overview, current models of angular momentum evolution (e.g. Bouvier et al. 1997; Allain 1998) suggest that stars rotating more rapidly on the ZAMS had a short-lived disk with a correspondingly shorter disk-locking time during their pre-main sequence phase than did their more slowly rotating counterparts. In addition, these stars may have had a higher initial angular momentum. However, after arrival on the ZAMS, models suggest that fast rotators spin down even more rapidly due to a more efficient magnetized wind (Kawaler 1988), that, in turn, dominates the angular momentum evolution of solar-type stars. As a consequence, solar-type stars should converge to the same rotation velocities at the age of the Sun (or M67) independent of their ZAMS rotation rates. This scenario would imply that magnetic

braking did not operate as efficiently in S1452 as in the other sun-like stars in our sample.

An additional perspective is provided by Bouvier (2008) who considers the effects of stellar rotational history on lithium depletion. In particular, Bouvier (2008) finds that rotational mixing is governed by the rotational shear at the base of the convective envelope, which, in turn, depends on the degree of core-envelope coupling. While this model is primarily applicable during the first ~ 1 Gyr in solar-type stars, the potential extension of the hypothesis of core-envelope decoupling to main sequence rotational evolution may be briefly considered. The result in his models is that lithium is more severely depleted in slow rotators on the ZAMS than fast rotators because slow rotators are characterized by stronger core-envelope decoupling that in a non-specific way leads to more efficient rotation-induced mixing. Conversely, fast rotators have less rotational shear in this model with correspondingly less efficient rotational mixing and, as a result, a lower rate of lithium depletion. In this regard, the recent investigation of candidate "solar twins" in M67 by Pasquini et al. (2008) is relevant.

In particular, the more rapidly rotating S1452 has a higher lithium abundance at $\log N(\text{Li}) = 1.0$ than do 7 of the 10 best solar twin candidates identified by Pasquini et al. (2008). This would suggest in the above model context of rotation-induced mixing that a spin-down with core-envelope decoupling dominated the rotational evolution of the solar twins. However, we note the important caveat that S1452 is slightly warmer than the solar twins. Therefore, it should not be surprising on this basis alone that the lithium depletion rate would be higher in the solar twins than in S1452.

A more appropriate comparison is with M67 stars characterized by estimated effective temperatures that are closer to that of our object. In this regard, S1452 has a lower lithium abundance than most of the stars in its bin of effective temperature between 5900 K to 5950 K. Furthermore, of the seven stars in our Table 1 that are in common with Pasquini et al. (2008), five have Li abundances greater than S1452 and two have lower abundances that are sun-like. These objects are slow rotators—an assertion that is supported by our measured upper limits of $v \sin i \lesssim 2 \text{ km s}^{-1}$ and their sun-like HK values. Furthermore, they have slightly lower effective temperatures which would suggest a relatively larger lithium depletion rate than in S1452.

Therefore, it seems unlikely in the above model context that there was a prolonged period on the main sequence of decoupled core-envelope spin-down for the slow rotators and, conversely, an extended period of coupled core-envelope rotational evolution for objects such as S1452. Moreover, the hydrodynamic or magnetohydrodynamic processes involved in any core-envelope decoupling and their association with the mixing of chemical species remain to be developed in the model advanced by Bouvier (2008). At this point, it would seem that the most natural qualitative explanation of the relatively higher rotational velocity of S1452 is that wind braking is less efficient in this object possibly as a result of a field configuration that is dominated by higher multipole moments,

which would also account for the higher level of chromospheric activity. But why this object should differ in this way from the other solar-type stars in M67 in its rotational evolution is not at all clear. We only note that S1452 is the earliest star in the sample ($B - V = 0.62$ while all others have $B - V = 0.63 - 0.67$). Hence, its higher rotation rate could be a natural consequence of a mass-dependence for rotational evolution on the M67 main sequence. A more extensive $v \sin i$ survey, particularly in a narrow color bin centered on the color of S1452, would have to be performed to further examine this possibility.

7. CONCLUSIONS

We find on the basis of the analysis of high resolution spectra of a subset of solar-type stars from the H & K survey of these objects in M67 by Giampapa et al. (2006) that stars with levels of chromospheric activity within the range of the contemporary cycle appear to have rotational velocities that are solar-like. At least one solar-type star with an HK index well in excess of the modern solar maximum is rotating more rapidly. Specifically, we measured a value for the projected rotation velocity of Sanders 1452 of $v \sin i = 4 \pm 0.5 \text{ km s}^{-1}$, or more than twice the solar equatorial rotation velocity. Another object in our sample, Sanders 747, is found to be a spectroscopic binary and is likely characterized by more rapid rotation than the Sun in at least one of its components. In view of these results, we conclude that the occurrence of high-activity levels in excess of solar maximum values for solar-type stars in M67 is most likely due to relatively faster rotation rather than to an excursion of a solar-like cycle to high values at solar rotation rates. Based on the correlation found between relative chromospheric emission and mean brightness variations we estimate an upper limit of about 0.2% in the level of broad-band variability in solar-type stars at solar ages and, by inference, in the Sun itself.

After a consideration of current models for angular momentum evolution for low mass stars, we tentatively attribute the more rapid rotation of solar-age stars such as Sanders 1452 to a reduced efficiency of braking due to a magnetized wind. Alternatively, the rapid rotation also could result simply from the particular mass-dependence of rotational braking in M67, as is seen in other clusters. A more comprehensive $v \sin i$ survey in M67 with specific emphasis on stars slightly warmer than the Sun will have to be performed to explore this hypothesis further.

The results presented in this investigation were based on observations obtained at the European Southern Observatory, Paranal, Chile, PID 080.D-0139. A.R. has received research funding from the DFG as an Emmy Noether fellow (RE 1664/4-1). The data utilized herein from the FTS instrument operated at the NSO/Kitt Peak McMath-Pierce Solar Telescope Facility were produced by NSF/NOAO. We acknowledge partial support of the publication of this work by a grant from the NASA/Astrobiology Institute to the University of Arizona and the NOAO.

REFERENCES

- Baliunas, S. L., 1995, ApJ, 438, 269
Barnes, S.A., 2007, ApJ, 669, 1167
Bonanno, A., Schlattl, H., & Patérno, L., 2002, A&A, 390, 1115
Bouvier, J., 2008, A&A, 489, L53
Bouvier, J., Forestini, M. & Allain, S., 1997, A&A, 326, 1023
Foukal, P. & Lean, J. 1990, Science, 247, 556
Giampapa, M.S., Hall, J.C., Radick, R.R., & Baliunas, S.L., 2006, ApJ, 651, 444
Gray, D.F., 2005, The Observation and Analysis of Stellar Photospheres, Cambridge University Press
Jirikovic, J. L. & Damon, P. E., 1994, Climatic Change, 26, 309
Kawaler, S. D., 1988, ApJ, 333, 236
Kenyon, S.J., & Hartmann, L., 1995, ApJS, 101,117
Kupka F., Piskunov N.E., Ryabchikova T.A., Stempels H.C., Weiss W.W., 1999, A&AS, 138, 119
Kurucz, R.L., Furenlid, I., Brault, J., & Testerman, L.. National Solar Observatory Atlas No. 1, June 1984
Lockwood, G. W., Skiff, B. A. & Radick, R. R., 1997, ApJ, 485, 789
Pace, G. & Pasquini, L., 2004, A&A, 426, 1021
Pallavicini, R., Golub, L., Rosner, R. & Vaiana, G. S., 1981, ApJ, 248, 279
Pasquini, L., Biazzo, K., Bonifacio, P., Randich, S. & Bedin, L. R., 2008, A&A, 489, 677
Pizzolato, N., Maggio, A., Micela, G., Sciortino, S. & Ventura, P., 2003 A&A, 397, 147
Radick, R. R., Lockwood, G. W., Skiff, B. A. & Baliunas, S. L., 1998, ApJS, 118, 239
Reiners, A., & Schmitt, J.H.M.M., 2003a, A&A, 398, 647
Reiners, A., & Schmitt, J.H.M.M., 2003a, A&A, 412, 813
Skumanich, A., 1972, ApJ, 171, 565
VandenBerg, D. A. & Bridges, T. J., 1984, ApJ, 278, 679
Yadav, R. K. S., Bedin, L. R., Piotto, G. et al., 2008, A&A, 484, 620